*Int. J. Electrochem. Sci.*, 7 **(2012)** 7935 - 7947

International Journal of
ELECTROCHEMICAL
SCIENCE
www.electrochemsci.org

# An Amperometric Biosensor Based on Direct Immobilization of Horseradish Peroxidase on Electrochemically Reduced Graphene Oxide Modified Screen Printed Carbon Electrode

*Selvakumar Palanisamy, Binesh Unnikrishnan, Shen-Ming Chen*[*]

Electroanalysis and Bioelectrochemistry Lab, Department of Chemical Engineering and Biotechnology, National Taipei University of Technology, No. 1, Section 3, Chung-Hsiao East Road, Taipei 106, Taiwan, ROC
[*]E-mail: smchen78@ms15.hinet.net

*Received:* 10 July 2012 / *Accepted:* 5 August 2012 / *Published:* 1 September 2012

In this work we report the synthesis of graphene oxide – horseradish peroxidase biocomposite (GO-HRP) by a solution method without using any cross-linkers. Then, the GO-HRP biocomposite was drop casted on a screen printed carbon electrode (SPCE) followed by the electrochemical reduction to reduced graphene oxide-HRP (ERGO-HRP) composite. The ERGO-HRP modified SPCE showed good electroanalytical properties towards the amperometric determination of $H_2O_2$. The film has been characterized by scanning electron microscopy (SEM) and electrochemical impedance spectroscopy (EIS). Both the studies revealed the effective immobilization of HRP on ERGO. The SPCE/ERGO-HRP showed a linear range of detection of 9 – 195 μM. The electrode also detects $H_2O_2$ in real sample solutions with appreciable accuracy.

**Keywords:** Horseradish peroxidase, $H_2O_2$, graphene oxide, reduced graphene oxide, amperometry, immobilization

## 1. INTRODUCTION

Hydrogen peroxide is an excellent oxidizing agent. Hence, it is widely used in organic synthesis and pharmaceutical industries, and used as cleaning and bleaching agents in many textile industries. $H_2O_2$ is also an important component in disinfectants, cleaning and antiseptic solutions for domestic use due to its antimicrobial property [1]. 3% $H_2O_2$ (v/v) is commonly used in many commercially available contact lens disinfectant solutions. So, $H_2O_2$ is released to the environment from the above mentioned activities. $H_2O_2$ is also released to the water resources by thunder and

lightning [2]. Researches show that the $H_2O_2$ concentration in rain water is increased by five times after thunder and lightning [3,4]. $H_2O_2$ can also cause some damages to brain and affects the central nervous system [5]. Therefore, $H_2O_2$ determination in environmental samples, biological samples, food samples, industries etc. are important [6,7]. Moreover, in biological systems $H_2O_2$ is produced by some biochemical reactions catalyzed by various enzymes. Therefore, by measuring the $H_2O_2$ the biochemical reactions can be determined indirectly [8]. Enzyme based biosensors have been a good choice due to their high selectivity [9] 10, 11]. Heme group containing proteins and enzymes are widely used for electrochemical reduction and determination of $H_2O_2$.

Horseradish peroxidase (HRP) is a glycosylated plant peroxidase and it can catalyze the reduction reaction of hydrogen peroxide [12]. In peroxidase based biosensors, $H_2O_2$ is reduced at low over potential due to the direct electron transfer between the electrode surface and HRP redox center [13]. Hence it is widely used in enzyme based amperometric biosensors [14-22]. However, the redox center or HRP is embedded in the protein matrix, which reduces the electrical conductivity of the enzyme and shows poor electron transfer rates. Since the redox center is hidden inside the protein matrix of the enzyme, it can avoid interference of many molecules with large size. So, a fast transfer of electron from the redox cite to the electrode is very important, which can be achieved by the use of nanomaterials. Direct electron transfer of HRP has been achieved at gold nanoparticles conjugate [23]. Gold nanoparticles can enhance the electron transfer between electrode and peroxidase [24]. Carbon nanotube also provide a suitable medium for electron transfer for HRP [25]. Cao et al. reported that HRP immobilised on nano-Au-poly 2,6-pyridinediamine showed higher electron transfer resistance than that of nano Au modified electrode [26].

Recently, graphene has attracted tremendous attention for HRP immobilization due to its functional and electrochemical and electrical properties. HRP has been immobilized on graphene oxide (GO) and applied for the removal of phenolic compounds [27]. While Lu et al. immobilized HRP on single layer graphene platelet for $H_2O_2$ biosensor application [28] which showed good performance. Graphene is an inexpensive material with good mechanical, electrical and thermal properties [29,30]. The large surface to volume ratio and biocompatibility are attractive parameters for its potential application in the fabrication of electrochemical biosensors [31]. It is difficult to prepare a uniform dispersion of graphene in aqueous solution due to its hydrophobic character. While GO is highly soluble in water because of the presence of remarkable amount of oxygen containing functional groups on its edge plains and surface. Also, the functional groups are useful for anchoring enzymes. Li et al. demonstrated the immobilization of HRP on electrochemically reduced graphene oxide (ERGO-HRP) [32]. So far no reports are available for the preparation of GO-HRP composite followed by electrochemical reduction to produce ERGO-HRP. Our previous report proves that the immobilization of glucose oxidase on GO followed by electrochemical reduction has many advantages in fabrication of biosensors [33]. In this work we report the synthesis of GO-HRP composite by a solution method. Then the GO-HRP has been electrochemically reduced to ERGO-HRP composite for the amperometric determination of $H_2O_2$.

## 2. EXPERIMENTAL

### *2.1 Apparatus*

The surface morphology characterization of the films were done by Scanning electron microscopy (SEM) using a Hitachi S-3000 H Scanning Electron Microscope. Electrochemical impedance spectroscopy (EIS) measurements were done using IM6ex ZAHNER (Kroanch, Germany). A conventional three electrode system with modified screen printed carbon electrode (SPCE) (Zensor, area: 0.196 $cm^2$) as working electrode, a thin Pt wire as counter electrode and Ag/AgCl (sat. KCl) as reference electrode was used. The cyclic voltammetric experiments were carried out using a CHI 750A electrochemical workstation. CHI 750A with an Analytical rotator MSRX (PINE Instruments, USA) was used for amperometric experiments.

### *2.2. Reagents and Materials*

Graphite powder with 98% purity and horseradish peroxidise were obtained from Sigma Aldrich. 30% $H_2O_2$ solution was from Wako pure chemical industries, Ltd. 0.1 M phosphate buffer solution (PBS) was prepared from 0.1 M $Na_2PO_4$ and $NaH_2PO_4$ in doubly distilled water and the pH was adjusted to 7. Inert atmosphere was set by passing $N_2$ over the solution during the electrochemical experiments. All the experiments were conducted at ambient temperature (25ºC ± 2ºC).

### *2.3 Fabrication of SPCE/ERGO-HRP modified electrode*

Graphite oxide was prepared from graphite platelets by modified Hummers' method following the procedures reported earlier [34, 35, 36]. Then, 0.5 mg/mL graphite oxide dispersion was prepared in deionized water and it was mechanically exfoliated by ultrasonication for 2 h to get GO solution. The prepared GO solution was used for electrode modification. For the fabrication of the ERGO-HRP composite modified electrode, 40 µL of GO solution (0.5 mg/mL) and 60 µL of HRP solution (10 mg/mL in 0.1M PBS, pH 7) were sonicated (30 min) in a vial to produce GO-HRP composite. Then, 10 µL of the GO-HRP composite was drop casted onto SPCE and allowed to dry at room temperature and rinsed with deionized water. The GO-HRP modified electrode (SPCE/GO-HRP) was transferred to $N_2$ saturated PBS (pH 5.0) solution. The GO-HRP film was then electrochemically reduced to ERGO-HRP by continuous potential cycling [28] (15 cycles) from 0 to – 1.5 V at a scan rate of 50 $mVs^{-1}$ by CV.

## 3 RESULTS AND DISCUSSION

### *3.1. Immobilization of HRP and electrochemical reduction of GO to ERGO in a single step*

Fig. 1 represents the electrochemical reduction process of GO. The cyclic voltammogram of the reduction process of GO on SPCE is shown in Fig. 1(A). In the first cycle, a broad cathodic peak with an onset potential of –0.8 V was observed, attributed to the reduction of oxygen functionalities of GO

[28]. The reduction current decreases significantly in the consecutive cycles. The modified electrode is noted as SPCE/ERGO. It should be noted, GO has many reactive functional groups such as ketone, quinine, carboxylic acid, hydroxyl, etc., Upon dispersing HRP in GO solution, the GO functionalities at the edge planes can easily bind with the free amino groups of HRP through covalent linkage.

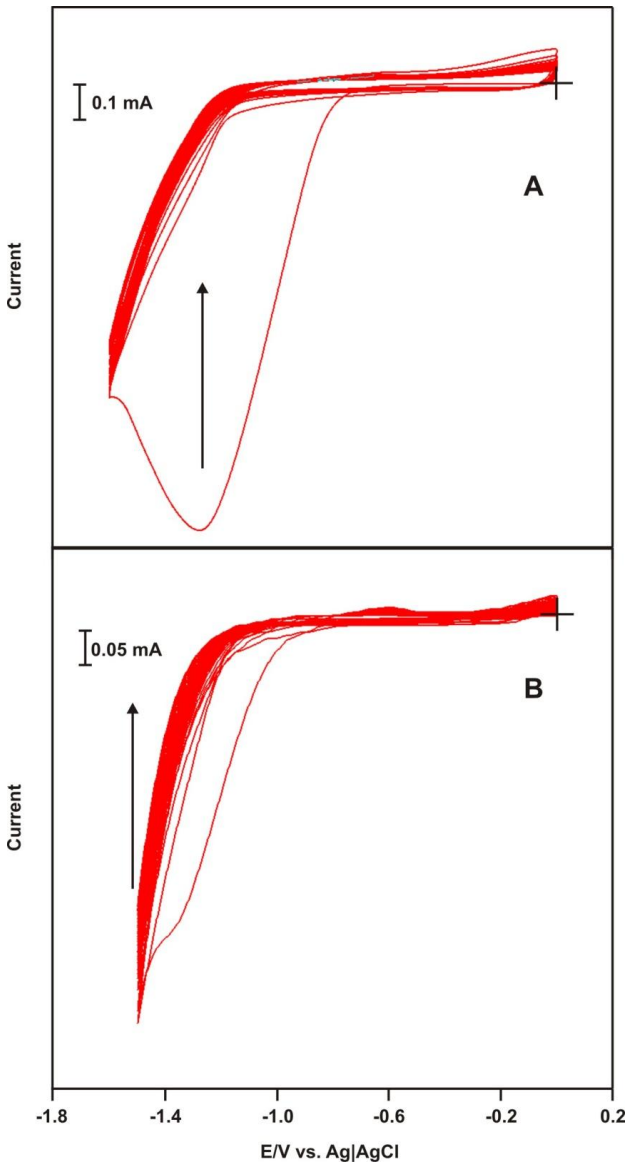


**Figure 1.** Cyclic voltammograms obtained for A) GO modified SPCE and B) GO-HRP modified SPCE in $N_2$ saturated pH 5. Scan rate: $0.05Vs^{-1}$.

Lysine present in the HRP has free primary amine group without any peptide linkage, and it can involve in coupling reaction [37]. The other amino acids present in the HRP such as alanine, cysteine, glycine, etc., do not have any free carboxylate group or primary amine group without peptide linkage, so they do not involve in coupling reaction. Therefore, HRP immobilized both by entrapment as well as by covalent linkage. Similarly, the as-prepared GO-HRP was electrochemically reduced in

the same potential range and number of cycles. It can be seen form Fig. 1(B) that the immobilization of HRP on GO by entrapment and covalent linkage decrease in the reduction peak current during the first cycle of GO-HRP reduction. This could be due to the less availability of surface oxygen functionalities on GO, as they are covalently linked with the free amino groups of HRP.

*3.2 EIS studies of various films*

Conducting polymers, polyelectrolytes, enzymes, proteins, nanomaterials or semiconducting materials coated on the electrode surface change the double layer capacitance and interfacial electron transfer resistance of the corresponding electrode. Impedance spectroscopy can reveal the interfacial changes due to the surface modification of electrodes [38]. The electrochemical impedance properties of the bare SPCE, HRP, ERGO, ERGO-HRP modified SPCE are recorded in 5mM $Fe(CN)_6^{3-}$ /$Fe(CN)_6^{4-}$ in PBS and are represented as Nyquist plot ($Z'$ vs. Z'') in fig. 2. The upper inset in Fig. 2 represents the GO modified SPCE. Lower inset in Fig. 2 shows the Randles equivalence circuit model used to fit the experimental data.

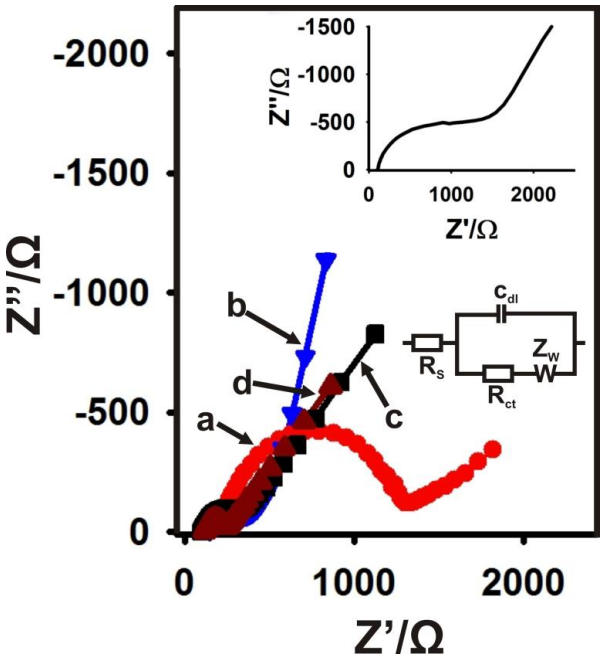


**Figure 2.** EIS of a) SPCE/HRP, b) bare SPCE, c) SPCE/ERGO, d) SPCE/ERGO-HRP in 5mM $Fe(CN)_6^{3-}$/$Fe(CN)_6^{4-}$ in 0.1 M PBS (pH 7). Applied AC voltage: 5mV, frequency: 0.1 Hz to 100 kHz. Upper inset is the EIS spectrum of SPCE/GO. Lower inset: Randles equivalence circuit model

Where $R_s$ is the electrolyte resistance, $R_{ct}$ is charge transfer resistance, $C_{dl}$ double layer capacitance and $Z_w$ is Warburg impedance. The semicircle appeared in the Nyquist plot indicates the parallel combination of $R_{et}$ and $C_{dl}$ resulting from electrode impedance [39]. The semicircles obtained at lower frequency represent a diffusion limited electron transfer process and those at higher frequency

represent a charge transfer limited process. As can be seen from Fig. 2 HRP modified SPCE (curve a) shows large semicircle indicating a high electron transfer resistance of the HRP film. This is due to the poor electrical conducting property of HRP. ERGO (curve c) and ERGO-HRP (curve d) modified SPCE show semicircles with small diameters indicating a lower electron transfer resistance due to the better electrical conducting property of ERGO. GO modified SPCE shows a larger semicircle showing a large electron transfer resistance (upper inset to Fig. 2) which is much higher than that of bare SPCE (curve b). This is due to the poor electrical conducting property of GO. Therefore, the electrochemical reduction of GO to ERGO and the presence of HRP on the film is one again confirmed by the above findings.

*3.3. Surface morphology characterization of various electrodes*

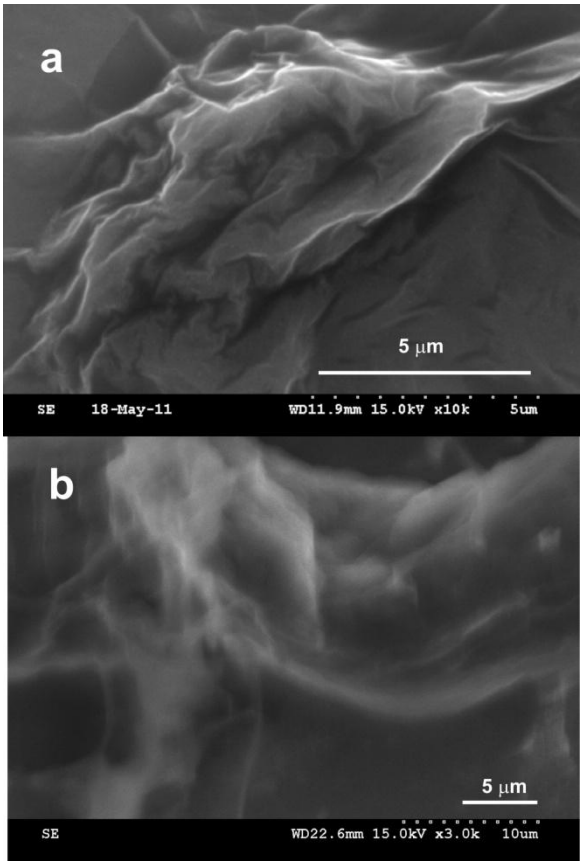


**Figure 3.** SEM images of ERGO and ERGO-HRO composite

The surface morphology of the ERGO and ERGO-HRP composite were studied by SEM. The ERGO and ERGO-HRP composite were prepared as per the procedure mentioned in sec. 2.3. Fig. 3 (a) shows the SEM images of ERGO with wrinkled and folding structures on the ERGO sheets. While HRP immobilized ERGO shows a thick surface where, the wrinkles and folding are occupied by the enzyme molecules (Fig. 3b). The difference between the surface morphology of the two materials suggests that HRP has been immobilized on the ERGO to form ERGO-HRP composite.

*3.4. Direct electrochemistry of HRP*

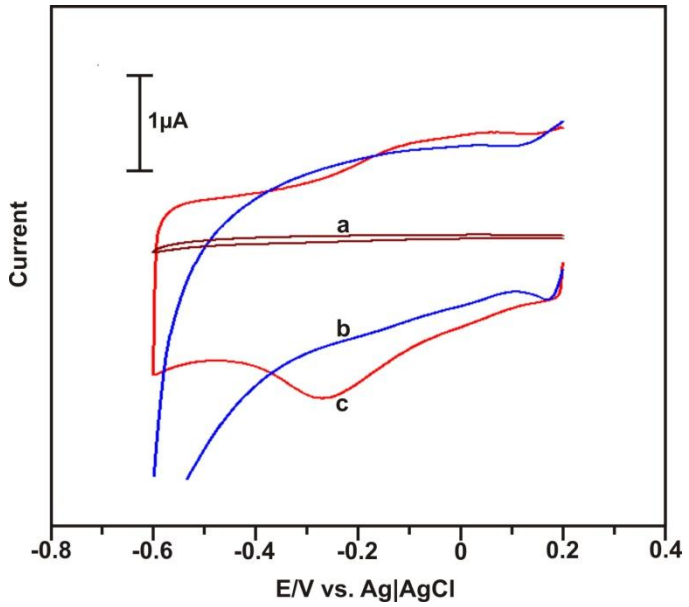


**Figure 4.** Cyclic voltammograms of a) bare SPCE, b) GO-HRP and c) ERGO-HRP modified film modified SPCEs in $N_2$ saturated PBS at the scan rate of 50 mV $s^{-1}$.

Electrochemical behavior of bare SPCE, GO-HRP, ERGO-HRP films modified SPCE were investigated using CV in $N_2$ saturated PBS at the scan rate of 50 mV $s^{-1}$ (Fig. 4). Curve (a) is the cyclic voltammogram of bare SPCE. Curve (b) represents the cyclic voltammograms of GO-HRP which does not show any significant peaks for HRP redox couple in the given potential range. Curve (c) shows the cyclic voltammetric response of ERGO-HRP film which shows a redox couple with the anodic peak appearing at –105 mV and the cathodic peak appearing at –260 mV. Since the peak potential difference ($\Delta E_p$) is well above 59 mV, the redox couple is electrochemically quasi-reversible. This redox couple ($Fe^{III/II}$) is due to the redox reaction of the heme group present in the HRP. This result validates the direct electron transfer between the HRP and the electrode surface. Our previous report on immobilization of glucose oxidase on ERGO suggests that the possible reason for the direct electron transfer is due to the presence of the HRP molecules at the closer vicinity of ERGO due to the cross linking between HRP and ERGO and entrapment of HRP in ERGO matrix [32]. Thus, ERGO facilitates the electron transfer between the active site of HRP to the electrode. The surface coverage concentration ($\Gamma$) of HRP at SPCE/ERGO-HRP has been calculated using the formula $\Gamma = Q/nFA$, where Q is the charge in coulombs, n is the number of electrons which is one for the $Fe^{(III/II)}$ redox couple of HRP, F is Faraday constant and $A$ is the area of the electrode. The $\Gamma$ value of HRP on ERGO-HRP modified SPCE has been calculated as $7.32 \times 10^{-10}$ mol $cm^{-2}$. The very large surface area of the ERGO provides more space for high enzyme loading.

The effect of scan rate on the redox peaks of ERGO-HRP has been investigated in $N_2$ saturated PBS (pH 7) in the scan rate range 10 – 100 $mVs^{-1}$. The cyclic voltammograms obtained for ERGO-HRP composite modified SPCE is given in Fig. 5. Both anodic ($I_{pa}$) and cathodic ($I_{pc}$) peak currents increase linearly with increase in scan rates. The linear dependence of peak currents with the scan rate

is given in the inset of Fig. 5. The linear regression equation for the anodic peak current can be written as $I_{pa}$ (μA) = 0.0206 ν + 0.7844, $R^2$ = 0.9934 and for cathodic peak current $I_{pc}$ (μA) = -0.0631 ν - 0.3774, $R^2$ = 0.9917. Where, ν is the scan rate in $mVs^{-1}$. Therefore, the redox reaction occurring at ERGO-HRP modified SPCE is a surface-confined electrochemical process.

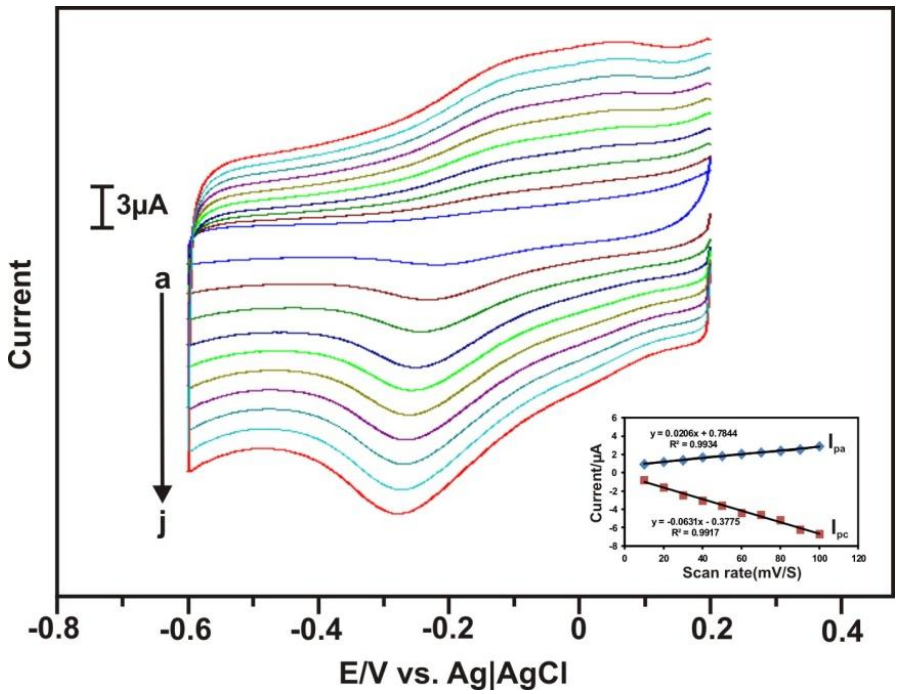


**Figure 5.** Cyclic voltammograms obtained for SPCE/ERGO-HRP in $N_2$ saturated pH 7 PBS at different scan rates. A → J: 10 → 100 $mVs^{-1}$. The inset shows the calibration plot for $I_{pa}$ and $I_{pc}$ vs. scan rate.

The electron transfer rate constant ($k_s$) for HRP at GCE/ERGO-HRP is calculated using the Laviron equation (1) [40] at higher scan rates.

$$\text{Log } k_s = \alpha \text{ Log } (1 - \alpha) + (1 - \alpha)\text{Log } \alpha - \text{Log}(RT/nFv) - \alpha\ (1 - \alpha)nF\Delta E_p/(2.3RT) \quad (1)$$

Where, $R$ is the universal gas constant (8.314 J $mol^{-1}$ $K^{-1}$), $T$ is the room temperature (298.15 $K$) and $\Delta E_p$ is the peak separation of the $Fe^{(III/II)}$ redox couple. α value is assumed as ≈0.5 and the number of electrons transferred is considered as 1. The $k_s$ value of HRP is calculated as 1.7 $s^{-1}$ indicating appreciable electron transfer kinetics process.

*3.5 Influence of pH*

The influence of pH on the redox behavior of SPCE/ERGO-HRP in various buffer solutions (pH, 1, 4, 5, 7, 9, 11 and 13) were also investigated in this study. The pH study results are shown in Fig. 6.

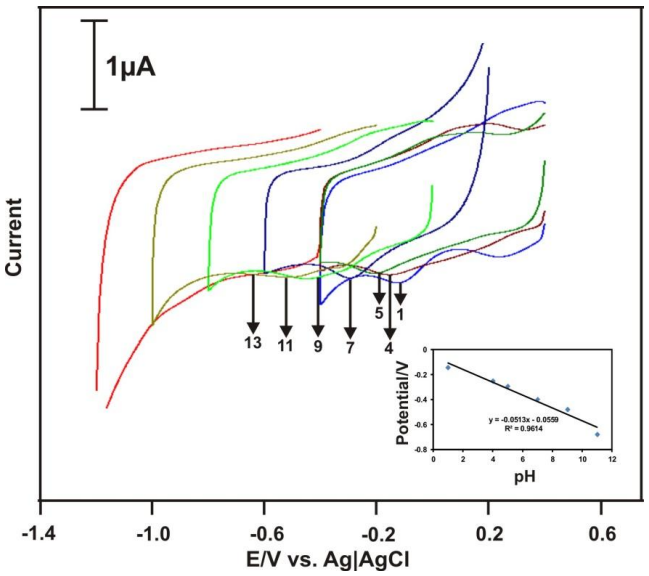


**Figure 6.** Cyclic voltammograms recorded for SPCE/ERGO-HRP in various $N_2$ saturated pH solutions separately. Inset shows the dependence of peak currents with pH.

Quasi-reversible redox peaks corresponding to $Fe^{(III/II)}$ redox process of HRP was observed in the pH range between 1 and 11. Significant peak was not observed in pH 13. This might be due to the loss of enzyme activity in the higher pH solution. The dependence of the formal potential $E°'$ with pH is given in the inset of Fig. 6. $E°'$ of the $Fe^{(III/II)}$ redox couple of HRP exhibits a linear dependence on pH. The $E°'$ values show a negative shift with increase in pH with a slope value of -51 mV $pH^{-1}$. This slope value is close to the theoretical value of -59 mV $pH^{-1}$ for an equal number of electron and proton transfer process.

### *3.6 Electrocatalysis of $H_2O_2$ at ERGO-HRP modified SPCE*

The electrocatalytic activity of ERGO-HRP film modified SPCE towards $H_2O_2$ reduction has been investigated using CV experiments. Fig. 7 shows the cyclic voltammograms obtained for various concentration of $H_2O_2$ at SPCE/ERGO-HRP in $N_2$ saturated PBS (pH 7). As shown in Fig. 7 ERGO-HRP film exhibits redox couple in the absence of $H_2O_2$ and the reduction peak current increases with the addition of $H_2O_2$. The calibration plot of linear dependence of current with the concentration of $H_2O_2$ is given in the inset of Fig. 7. The linear regression equation can be written as $I_{pc}$ (µA) = - 0.1017 C (µM) –0.2478, $R^2$ = 0.9777. The composite film thus exhibits promising electrocatalytic activity towards $H_2O_2$ which could be attributed to the good biocompatibility of the immobilized HRP as well as the synergistic effect of ERGO matrix for $H_2O_2$.

In order to understand the reproducibility of the biosensor, four individual electrodes were prepared and the currents were measure for 3 µM $H_2O_2$ in $N_2$ saturated PBS (pH7). The relative standard deviation was 3.27%. The repeatability of the biosensor has been tested by measuring the

current in four different solutions containing 3 μM $H_2O_2$ after rinsing the electrode with PBS after each measurement. The sensor shows an R.S.D of 4.53%.

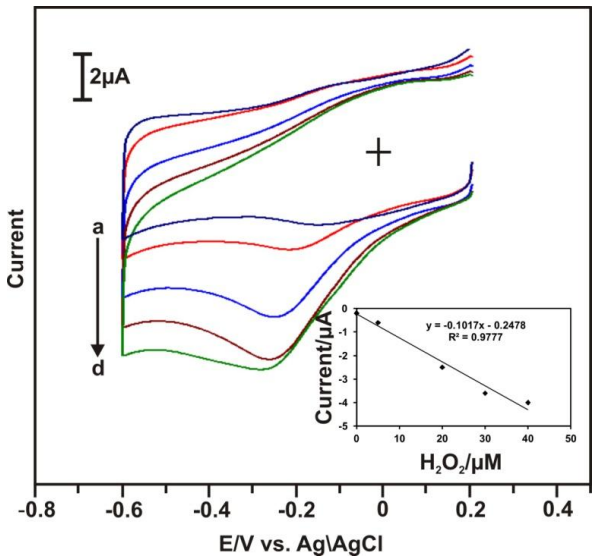


**Figure 7.** Cyclic voltammograms of SPCE/ERGO-HRP at different concentrations of $H_2O_2$ in $N_2$ saturated PBS (pH7) a → d: 0.0, 5, 20, 30, and 40μM. Scan rate: 50 $mVs^{-1}$. Inset shows the calibration plot for Peak current vs. concentration of $H_2O_2$.

### *3.7. Amperometric response of $H_2O_2$ at ERGO-HRP composite modified rotating disc electrode*

The amperometric response of $H_2O_2$ at ERGO-HRP modified rotating disc glassy carbon electrode was studied in $N_2$ saturated PBS (pH 7). During the amperometric experiments the electrode potential was held at –0.28 V and the $N_2$ saturated PBS was continuously stirred at 1200 RPM. Inert atmosphere was created above the solution by passing $N_2$ gas over the solution. Aliquots of $H_2O_2$ were successively injected into the supporting electrolyte solution with constant interval (50 s). For every addition of $H_2O_2$ a quick response was obtained for the reduction of $H_2O_2$.

The current decreases linearly with time up to 1500 s and then tend to become plateau. An enlarged view of the amperometric response of $H_2O_2$ is given in the inset of Fig. 8. The plot of reduction current vs. concentration of $H_2O_2$ is given in the inset (b) of Fig. 8. The sensor shows a linear range of detection from 9 – 195 μM. The sensitivity of the sensor is 0.09 μA $\mu M^{-1}$ $cm^2$. In order to evaluate the affinity of immobilized HRP towards $H_2O_2$, the apparent Michaelis–Menten constant ($K_M^{app}$) has been calculated from the electrochemical version of the Lineweaver–Burk equation [41] as shown in Eq. (2).

$$1/I_{ss} = 1/I_{max} + K_M^{app}/(I_{max}\, C) \qquad (2)$$

Where $I_{max}$ and $I_{ss}$ are the currents measured for enzymatic product detection under substrate saturation and steady state, respectively for a given concentration, $C$. A plot of $1/I_{ss}$ vs. $1/C$ gave a

straight line for the concentrations above 0.2 mM showing a Michaelis-Menten kinetic mechamism. From the slope ($K_M^{app}/I_{max}$) and intercept ($1/I_{max}$) values $K_M^{app}$ value is calculated as 0.5 mM. The small $K_M^{app}$ value obtained indicates the high affinity of the immobilized HRP towards $H_2O_2$.

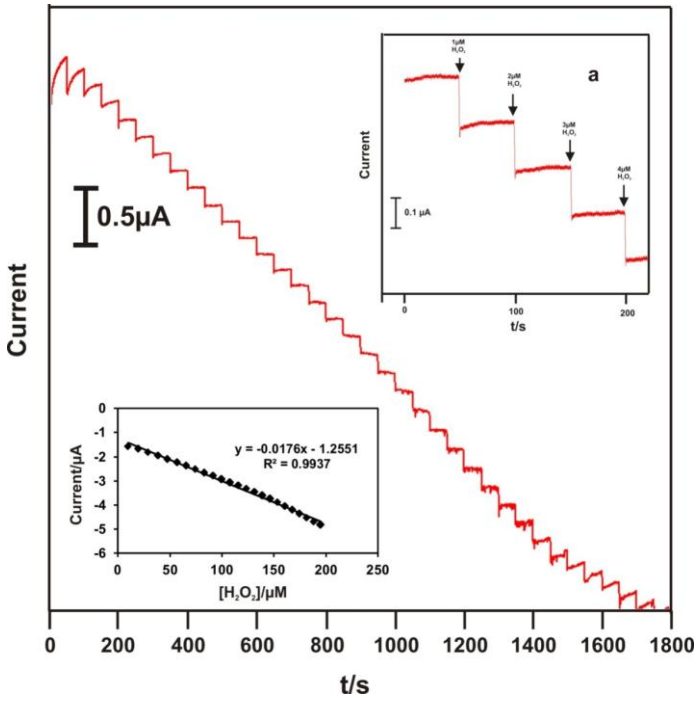


**Figure 8.** Amperometric response of $H_2O_2$ at ERGO-HRP modified rotating disc glassy carbon electrode in $N_2$ saturated PBS (pH 7). Applied potential: – 0.28V, rotation rate: 1200 rpm. Inset a shows the enlarged view of the amperometric response and b shows the calibration plot for peak current vs. concentration of $H_2O_2$.

*3.8 Real sample analysis*

In order to validate the practical feasibility of the developed $H_2O_2$ biosensor, it is applied to determine the $H_2O_2$ content of a commercial cleaning solution containing 3% $H_2O_2$ by i-t amperometry. The results are presented in Table 1.

**Table 1.** The recovery of the real sample analysis at the ERGO-HRP modified electrode

| Sample | Added $H_2O_2$ (μM) | Found $H_2O_2$ (μM) | Recovery (%) |
|---|---|---|---|
| 1 | 50.0 | 50.61 | 101.22 |
| 2 | 100.0 | 99.44 | 99.44 |
| 3 | 150.0 | 148.79 | 99.19 |

*3.9 Interferance*

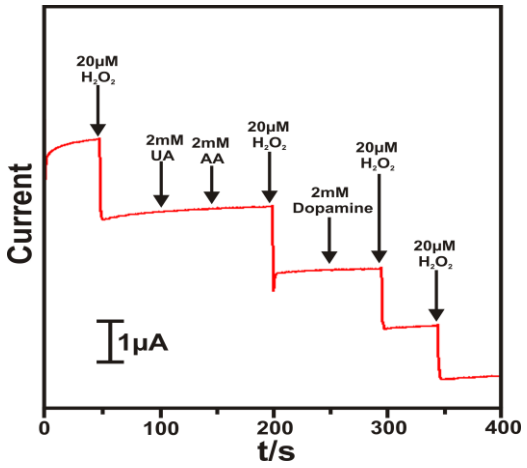


**Figure 9.** Amperometric response of $H_2O_2$, uric acid, ascorbic acid and dopamine at SPCE/ERGO-HRP in $N_2$ saturated PBS. Applied potential: -0.28 V. Rotation speed: 1200 rpm.

To understand the selectivity of the developed sensor, some common interfering species in biological samples have been tested. Common compounds such as dopamine, ascorbic acid and uric acid have been tested by amperometry in $N_2$ saturated PBS (pH 7). The amperometric response of $H_2O_2$ and the above mentioned compounds are presented in Fig. 9. The proposed sensor does not show any significant amperometric response for the ascorbic acid, uric acid or dopamine. Thus the result shows the HRP based biosensor is highly selective in detecting $H_2O_2$.

## 4. CONCLUSION

We demonstrated the fabrication of ERGO-HRP biocomposite from GO-HRP by electrochemical approach. The HRP immobilization process is facile and no cross-inker was used. The wide linear range, high selectivity and the good stability of this sensor can extend its practical applications further. The ERGO-HRP modified SPCE shows very good amperometric response towards $H_2O_2$ reduction with a sensitivity of 0.09 μA $\mu M^{-1}$ $cm^2$. The characterization of ERGO-HRP by various methods suggests that the fabrication process mentioned in this work can be employed for the fabrication of graphene based composites of a wide range of electrochemically important molecules with redox properties.

ACKNOWLEDGEMENT
The authors express their gratitude to Veerappan Mani for his help in synthesis and characterization of graphene oxide and reduced graphene oxide. This project was supported by the National Science Council and the Ministry of Education of Taiwan (Republic of China).

## References

1. E. Linley, S. P. Denyer, G. McDonnell, C. Simons and J. Y. Maillard, *J Antimicrob. Chemother.*, 67 ( 2012) 1589–1596.
2. Y. Komazaki, T. Inoue and S. Tanaka, *Analyst*, 126 (2001) 587.

3. Y. Deng and Y. Zuo, *Atmos. Environ.*, 33 (1999) 1469.
4. T. Tanaikai, A. Sakuragawa, and T. Okutani, *Anal. Sciences*, 16 (2000) 275.
5. E. A. Mazzio and K. F. A. Soliman, *J. Appl. Toxicol.*, 24 (2004) 99.
6. X. B. Lu, J. H. Zhou, W. Lu, Q. Liu and J. H. Li, *Biosens. Bioelectron.*, 23 (2008) 1236.
7. X. H. Shu, Y. Chen, H. Y. Yuan, S. F. Gao and D. Xiao, *Anal. Chem.*, 79 (2007).
8. Y. X. Ci and F. Wang, *J. Anal. Chem.*, 339 (1991) 46-49.
9. A. S. Rad, A. Mirabi, E. Binaian, H. Tayebi, *Int. J. Electrochem. Sci.*, 6 (2011) 3671 – 3683.
10. Y. H. Wu and S. S. Hu, *Microchim. Acta*, 159 (2007) 1.
11. L. Gorton, *Electroanal*., 7 (1995) 23.
12. H. B. Dunford, Heme Peroxidases; Wiley: New York, 1999.
13. S. V. Dzyadevych, V. N. Arkhypova, A. P. Soldatkin, A. V. Elskaya, C. Martelet , N. Jaffrezic-Renault, ITBM-RBM, 29 (2008) 171.
14. S. Ledru, N. Ruille and M. Boujtita, *Biosens. Bioelectron.*, 21 (2006) 1591.
15. J. Wang, L. Wang, J. Di and Y. Tu, *Talanta*, 77 (2009) 1454.
16. A. P. Periasamy, Y. H. Ho, and S. M. Chen, *Biosens. Bioelectron.*, 29(2011) 151-158.
17. A. P. Periasamy, S. Yang, S. M. Chen, *Talanta*, 87 (2011) 15-23.
18. S. W. Ting, A. P. Periasamy, S. M. Chen, R. Saraswathi, , *Int. J. Electrochem. Sci.*. 6 (2011) 4438-4453.
19. Y. L. Yang, B. Unnikrishnan, S. M. Chen, *Int. J. Electrochem. Sci.*. 6 (2011) 3743-3753
20. A. P. Periasamy, S. W. Ting, S. M. Chen, *Int. J. Electrochem. Sci.*. 6 (2011) 2688-2709.
21. J. Y. Yang, Y. Li, S. M. Chen, K. C. Lin, *Int. J. Electrochem. Sci.*. 6 (2011)2235-2245.
22. K. C. Lin, T. H. Tsai, S. M. Chen, *Biosens. Bioelectron.*, 26 (2010) 608-614
23. G. K. Ahirwal and C. K. Mitra, *Sensors* 9 (2009) 881-894.
24. J. J. Feng, G. Zhao, J. J. Xu and H.Y. Chen, *Anal. Biochem.*, 342 (2005) 280-286.
25. Y. Yin, Y. Lü, P. Wu and C. Cai, *Sensors* 5 (2005), 220-234.
26. S. Cao , R. Yuan, Y. Chai, L. Zhang, X. Li and F. Gao, *Bioprocess Biosyst. Eng.* 30 (2007) 71–78.
27. F. Zhang, B. Zheng, J. Zhang, X. Huang, H. Liu, S. Guo and J. Zhang, *J. Phys. Chem. C*, 114 (2010) 8469–8473.
28. Q. Lu, X. Dong, L. J. Li and X. Hu, *Talanta* 82 (2010) 1344–1348.
29. K. S. Novoselov, A. K. Geim, S. V. Morozov, D. Jiang, Y. Zhang, S. V. Dubonos, I. V. Grigorieva and A. A. Firsov, *Science* 306 (2004) 666-669.
30. A. K. Geim and K. S. Novoselov, *Nat. Mater*. 6 (2007) 183.
31. T. Kuila, S. Bose, P. Khanra, A. K. Mishra, N. H. Kim and J. H. Lee, *Biosens. Bioelectron.* 26 (2011) 4637-4648.
32. M. Li, S. Xu, M. Tang, L. Liu, F. Gao and Y. Wang, *Electrochim. Acta* 56 (2011) 1144-1149.
33. B. Unnikrishnan, S. Palanisamy and S. M. Chen, *Biosens. Bioelectron.*, (2012) http://dx.doi.org/10.1016/j.bios.2012.06.045.
34. W. S. Hummers. and R. E. Offeman, *J. Am. Chem. Soc*. 80 (1958) 1339.
35. H. L. Guo, X. F. Wang, Q. Y. Qian, F. B. Wang and X. H. Xia, ACS NANO 3 (2009) 2653-2659.
36. G. Wang, X. Shen, J. Yao and J. Park, *Carbon* 47 (2009) 2049-2053.
37. M. J. B. Wissink, R. Beernink, J. S. Pieper, A. A. Poot, G. H. M. Engbers and T. Beugeling, *Biomaterials* 22 (2001) 151-163.
38. E. Katz, I. Willner and *Electroanal.*, 15 (2003) 913.
39. H. O. Finklea, D. A. Snider and J. Fedyk, *Langmuir* 9 (1993) 3660.
40. Laviron, E., *J. Electroanal. Chem*. 101 (1979) 19–28.
41. R. A. Kamin and G. S. Willson, *Anal. Chem*., 52 (1980) 1198–1205.